Electronic Origin of Ultrafast Photoinduced Strain in BiFeO_{3}

Haidan Wen, Pice Chen, Margaret P. Cosgriff, Donald A. Walko, June Hyuk Lee, Carolina Adamo, Richard D. Schaller, Jon F. Ihlefeld, Eric M. Dufresne, Darrell G. Schlom, Paul G. Evans, John W. Freeland, and Yuelin Li

Phys. Rev. Lett. **110**, 037601 — Published 18 January 2013

DOI: 10.1103/PhysRevLett.110.037601

Electronic origin of ultrafast photoinduced strain in $BiFeO_3$

Haidan Wen,[1] Pice Chen,[2] Margaret P. Cosgriff,[2] Donald A. Walko,[1] June Hyuk Lee,[1] Carolina Adamo,[3] Richard D. Schaller,[4,5] Jon F. Ihlefeld,[6] Eric M. Dufresne,[1] Darrell G. Schlom,[3] Paul G. Evans,[2] John W. Freeland,[1] and Yuelin Li[1*]

[1] *X-ray Science Division, Argonne National Laboratory, Argonne, Illinois 60439, USA*

[2] *Department of Materials Science and Engineering & Materials Science Program, University of Wisconsin–Madison, Madison, Wisconsin 53706, USA*

[3] *Department of Materials Science and Engineering, Cornell University, Ithaca, New York 14853, USA*

[4] *Center for Nanoscale Materials, Argonne National Laboratory, Argonne, Illinois 60439, USA*

[5] *Department of Chemistry, Northwestern University, Evanston, Illinois 60208, USA*

[6] *Sandia National Laboratories, Albuquerque, New Mexico 87185, USA*

**ylli@aps.anl.gov*

PACS numbers: 77.55.Nv, 78.47.J-, 78.47.jb, 61.05.cp

Abstract

Above-bandgap optical excitation produces interdependent structural and electronic responses in a multiferroic $BiFeO_3$ thin film. Time-resolved synchrotron x-ray diffraction shows that photoexcitation can induce a large out-of-plane strain, with magnitudes on the order of half of one percent following pulsed-laser excitation. The strain relaxes with the same nanosecond time dependence as the interband relaxation of excited charge carriers. The magnitude of the strain and its temporal correlation with excited carriers indicate that an electronic mechanism, as rather than thermal effects, is responsible for the lattice expansion. The observed strain is consistent with a piezoelectric distortion resulting from partial screening of the depolarization field by charge carriers, an effect linked to the electronic transport of excited carriers. The non-

thermal generation of strain via optical pulses promises to extend the manipulation of ferroelectricity in oxide multiferroics to subnanosecond timescales.

The coupled degrees of freedom in complex oxides can be readily manipulated by light, providing new avenues for understanding and controlling fundamental physical properties. Within this broad range of materials, complex oxides with a built-in electrical polarization, including ferroelectrics and multiferroics, can respond to optical excitations through the interaction of photoinduced charge carriers with the spontaneous polarization. In $BiFeO_3$ (BFO), a room temperature magnetoelectric multiferroic [1–3], these responses include unidirectional photocurrents within individual polarization domains [4] and open-circuit photovoltages larger than the bandgap across ferroelectric domain walls [5,6]. Charge separation during the photovoltaic response in turn influences degrees of freedom conventionally associated with ferroelectricity: the magnitude of the spontaneous polarization and the electromechanical distortion of the lattice. As a result of these observations, photoinduced structural changes in ferroelectrics [7] and multiferroics [8,9] have been described as arising from the excitation of charge carriers. However, the timescales and mechanisms of processes that begin with the optical excitation and result in the subsequent structural distortion are largely unknown. Establishing the relationship between the concentration of optically excited charge carriers and the non-equilibrium distortion of the atomic-scale structure is essential for understanding photoinduced phenomena in strongly correlated systems.

In this Letter, we show that the strain induced by optical excitation of BFO is proportional to the population of optically excited charge carriers. The magnitude of this effect is sufficiently large that pulsed optical excitation can induce transient strain on the order of half of one percent. Time-resolved synchrotron x-ray diffraction measurements show that the strain develops within 100 ps and subsequently relaxes in several ns. The decay of the charge carrier population observed using ultrafast optical absorption spectroscopy occurs on an identical nanosecond

timescale. The correlation of the electronic and structural responses upon optical excitation provides insight into the mechanism of photoinduced strain. The distinct nanosecond decay time of the photoinduced strain allows it to be distinguished from the slower relaxation of thermal expansion. The large non-thermal component of the strain is consistent with either piezoelectric distortion due to screening of the depolarization field by photogenerated carriers or a direct modification of the crystal structure through populating the anti-bonding states of the transition metal.

Time-resolved x-ray diffraction experiments were performed under ambient conditions at beamline 7ID-C of the Advanced Photon Source [10]. BFO films with a thickness of 35 nm were grown by reactive molecular-beam epitaxy on (001) $SrTiO_3$ (STO) substrates through adsorption-controlled codeposition [11]. Optical excitation during the x-ray diffraction studies was provided by 50 fs laser pulses with a central wavelength of 400 nm, derived by frequency doubling the output of a Ti:sapphire laser system and synchronized to the x-ray pulses with an electronically adjustable time delay. Incident x-rays with a photon energy of 10 keV and pulse duration of 100 ps were focused to 50 μm full-width-half-maximum (FWHM) in diameter, overfilled by a 1 mm FWHM pump laser spot. Separate transient optical absorption measurements were performed at the Center for Nanoscale Materials. Optical absorption in the wavelength range from 400 to 750 nm was probed by a chirped 1 ps white-light pulse with time delays up to 7.2 ns after a 40 fs, 400 nm pump pulse. The magnitude of the laser excitation is reported in terms of the absorbed fluence. The penetration depth of 400 nm light in BFO is 32 nm [12], comparable to the thickness of the film.

A large expansion of the BFO out-of-plane lattice parameter *c* was observed upon photoexcitation, leading to a shift of the pseudo-cubic (002) reflection to lower Bragg angle, as

shown in Fig. 1a. Bragg peaks measured at pump-probe delays before the optical pulse are identical to measurements without laser excitation, indicating that the optically excited BFO lattice returns to its ground state within the interval between successive excitation pulses (0.2 ms). The photoinduced strain ($\Delta c/c$) measured 100 ps after the pump pulse reaches 4.1×10^{-3} for a laser fluence of 3.2 mJ/cm^2. In contrast, below-band-gap excitation using 800 nm laser pulses with similar laser fluence yielded no observable lattice change, suggesting an important role of electronic excitation. The (002) reflection is broadened from 0.22° to 0.25° FWHM at 100 ps after the optical excitation, possibly due to a strain gradient arising from the inhomogeneity of the optical excitation or from localized lattice distortion caused by the trapping of charges or the formation of polarons [13]. The total integrated intensity of the reflection remains constant throughout the relaxation processes.

The change of the Bragg angle of the BFO (002) reflection is shown as a function of pump-probe delay in Fig. 1b. The relaxation processes following excitation at three different pump fluences are fit by a bi-exponential decay with a fast time constant of 2.1 ± 0.2 ns and a slow time constant of 63 ± 35 ns. The time-resolution of the diffraction studies is limited by the 100-ps duration of the x-ray pulses and thus previously observed sub-ps responses to optical excitation seen in other oxide systems [7,14,15] are not resolved in Fig. 1b. To characterize the dependence of the structural distortion on the magnitude of the excitation, we measured the shift of the (002) reflection as a function of optical pump fluence at fixed time delays of 100 ps and 15 ns (Fig. 1c). The strain at both time delays is proportional to the pump fluence, in agreement with mechanisms in which the strain results from one-photon linear absorption of the above-band-gap radiation. The in-plane lattice constants measured using the BFO (113) peak are unchanged following optical excitation due to the epitaxial constraint provided by the substrate.

Transient optical absorption measurements were employed to understand the connection between the photoinduced strain and excited carriers by probing the dynamics of the carrier population in the excited states. A broad photoinduced absorption peak centered at 540 nm appears upon laser excitation (Fig. 2a). The strong increase in absorption after excitation (Fig. 2b, inset) arises from excited-state absorption of electrons in the conduction band and holes in the valence band [16]. The initial transient signal partially decays within 1 ps due to intraband relaxation. The ps-scale decay is followed by a slower decay of the induced absorption over several ns (Fig. 2b), as the concentration of charge carriers decreases due to carrier recombination. We have parameterized the carrier dynamics after 100 ps by a bi-exponential decay. Fits of three scans at various absorbed fluences each yield a fast time constant of 0.18 ± 0.06 ns and a slow time constant of 2.2 ± 0.1 ns.

The transient absorption measurements reveal the timescales associated with energy relaxation for photoexcited carriers in BFO. The initial absorption promotes carriers to excited states at energies far from the band edges. Energy in excess of the electronic bandgap is transferred to the lattice through the electron-phonon interaction and increases the lattice temperature within a period of several ps. The remaining photon energy relaxes mainly through radiative carrier recombination on a ns time scale, as evidenced by recent photoluminescence measurements [17]. The initial temperature rise of BFO lattice can be approximated by considering only the thermalization of the absorbed energy in excess of the bandgap, which gives rise to the temperature increase of BFO by 64 K following an optical pulse with fluence of 3.47 mJ/cm^2 (see Supplemental Material).

In order to determine the thermal contribution to the transient lattice expansion, we measured the thermal expansion coefficient using the shifts of the (001) and (002) BFO Bragg

reflections in which the temperatures of the substrate and BFO film were changed together between 25 and 155 °C. To compare with the present optical-excitation experiment, a modified thermal expansion coefficient for BFO must be defined to correct for the experimental difference that the laser excitation directly heats only the BFO film but not the substrate. The in-plane stress imparted by the room-temperature STO substrate on the laser-heated BFO film leads to additional out-of-plane expansion. Using a Poisson's ratio of 0.34 for BFO [18], the effective thermal expansion coefficient for out-of-plane expansion is experimentally determined to be $1.84\times10^{-5}\,K^{-1}$. The laser-induced temperature rise of 64 K thus leads to a strain of 1.2×10^{-3}. The thermal expansion represents only 27% of the 4.4×10^{-3} strain induced upon photoexcitation and is insufficient to account for the magnitude of the strain observed at sub-nanosecond time scales.

To correlate the structural response with the carrier dynamics, we compare the time dependence of the induced optical absorption and the induced strain (Fig. 3a). The induced optical absorption relaxes within several nanoseconds while the strain shows a long-lived component persisting beyond 14 ns. The deviation of the strain dynamics from the decay of the induced absorption at later time arises from the slow relaxation of the thermal expansion of the BFO due to thermal transport from the film to the substrate. To better illustrate the correlation between the photoinduced carrier population and strain, the strain can be plotted as a function of the change in optical density due to absorption by excited carriers (ΔOD) at each time, as in Fig. 3b. Since ΔOD measures the concentration of optically excited carriers, the linear relation between strain and ΔOD reveals a direct correlation between the measured strain and the photoinduced carrier concentration in BFO. The linear fits (solid lines, Fig. 3b) show a non-zero strain at ΔOD=0 due to the thermal contribution.

The time dependence of the photoinduced strain can be modeled by combining carrier-

induced strain and thermal expansion. The normalized strain is given by $S(t) = (1-a)S_c(t) + aS_q(t)$. The first term describes the dynamics of the carrier-induced strain shown as the red curve in Fig. 4, where $S_c(t)$ is a bi-exponential function that is proportional to the measured ΔOD. The second term describes the time-dependent thermal expansion as depicted by the green curve in Fig. 4, where $S_q(t)$ is proportional to the time-dependent temperature profile obtained by numerically solving a one-dimension thermal diffusion equation that describes the thermal transport processes in BFO/STO heterostructures (see Supplemental Material), similar to the treatment in Ref. [19]. The value of *a* represents the ratio of the thermally induced strain and the total measured strain at 100 ps, which equals to 0.27 for a pump fluence of 3.47 mJ/cm^2. By varying only one parameter, the interfacial conductance, the model (blue curve, Fig.4) fits well to the observed strain (triangle, Fig.4). Therefore, we conclude that the fast decay of the induced strain within 2 ns is dictated by the carrier dynamics, while the slow decay in tens of ns (measured time constant of 63 ± 35 ns) is governed by the thermal transport between the film and substrate [19,20].

The non-thermal component of the photoinduced strain can be described by a model in which photoinduced carriers are driven to the film surfaces by the depolarization field. This model has been previously proposed to explain the distortion of ferroelectric thin films after 100 ps following laser excitation [7]. In BFO film, the depolarization field along pseudocubic <001> directions arises to balance the external electric field induced by the out-of-plane component of the ferroelectric polarization along the <111> direction. The accumulation of charges at the surfaces due to the drift of excited carriers in the depolarization field creates a time-dependent electric field opposing the depolarization field along the out-of-plane direction. This transient electric field in turn drives the *c*-axis piezoelectric expansion. The electric field induced by

photoexcitation is proportional to the surface charge density, and thus proportional to the pump fluence, which could explain the linear response of the strain to the optical fluence shown in Fig. 2c. The transient field decreases as a result of reduction of surface charge density. Thus the induced strain relaxes at the same time scale of charge carrier recombination, supported by the agreement between the time constants that characterize the decay of induced strain and optical absorption.

The optically induced electric field can be estimated using the piezoelectric relationship between strain and electric fields. With a low-field piezoelectric coefficient d_{33} of 50 pm/V for BFO [21], the peak electric field is 880 kV/cm for a strain of 4.4×10^{-3}, which requires a surface charge concentration of 4 μC/cm^2. This is only 0.4% of the surface charge density that would arise if each optical photon absorbed in BFO excited one electron-hole pair that subsequently migrated to the film surface, the surface charge density. We suspect, therefore, that a significant number of charge carriers may be trapped locally by defects, domain walls [22] or as a result of Debye screening due to possible high charge concentration in BFO, rather than migrating to the interfaces of the BFO layer.

A quantitative analysis of dynamics of the screening of the depolarization field is complicated because the diffusion length and mobility of excited electrons in BFO are currently unknown. In addition, domains in which the ferroelectric polarization points along four pseudocubic diagonals coexist in the sample [23], making the electrostatic environment difficult to model. In the case in which the diffusion length and mobility of excited electrons in BFO are insufficient to provide the required screening, a mechanism of directly modifying the crystal structure by photoexcitation would be particularly important. Similar to the V-V bond dilation upon optical excitation in VO2 [24], the direct modification of crystal structure in BFO by

exciting anti-bonding electronic states of the transition metal could be an additional cause of photoinduced expansion of the BFO lattice as a result of the increase of bond distances.

In addition to providing fundamental insight into photoinduced structural dynamics, the demonstration of ultrafast optical manipulation of the piezoelectric strain has important implications. Because the initial thermal contribution to the photoinduced strain arises only from intraband relaxation of the excited carriers, the initial pulse of heat transferred to the lattice can be reduced to a negligible level by tuning the excitation photon energy closer to the band edge. More generally, large optically induced strain opens a new route for ultrafast strain engineering of multifunctional complex oxides. An induced transient strain on the order of half percent, when combined with epitaxial strain engineering, can drive a system across structural or magnetic phase boundaries, allowing an ultrafast strain to tune the functional properties of complex oxides. In addition, the large transient electric field can be used to apply an electric field across a BFO thin film without electrodes, opening new opportunities for elucidating the magneto-electric coupling in multiferroics and for manipulation of magnetism for spintronic applications [25,26].

Work at Argonne was supported by the U.S Department of Energy, Office of Science, and Office of Basic Energy Sciences, under Contract No. DE-AC02-06CH11357. Work at the University of Wisconsin was supported by the U. S. Department of Energy, Office of Basic Energy Sciences, Division of Materials Sciences and Engineering, through grant number DEFG02-10ER46147. Work at Cornell University was supported by Army Research Office through agreement W911NF-08-2-0032. Sandia National Laboratories is a multi-program laboratory managed and operated by Sandia Corporation, a wholly owned subsidiary of Lockheed Martin Corporation, for the U.S. Department of Energy's National Nuclear Security Administration under contract DE-AC04-94AL85000.

Reference:

[1] G. Catalan and J. F. Scott, Adv. Mater. **21**, 2463 (2009).

[2] R. Ramesh and N. A. Spaldin, Nature Mater. **6**, 21 (2007).

[3] W. Eerenstein, N. D. Mathur, and J. F. Scott, Nature **442**, 759 (2006).

[4] T. Choi, S. Lee, Y. J. Choi, V. Kiryukhin, and S.-W. Cheong, Science **324**, 63 (2009).

[5] S. Y. Yang, J. Seidel, S. J. Byrnes, P. Shafer, C.-H. Yang, M. D. Rossell, P. Yu, Y.-H. Chu, J. F. Scott, J. W. Ager, L. W. Martin, and R. Ramesh, Nature Nanotech. **5**, 143 (2010).

[6] J. Seidel, D. Fu, S.-Y. Yang, E. Alarcón-Lladó, J. Wu, R. Ramesh, and J. Ager, Phys. Rev. Lett. **107**, 126805 (2011).

[7] D. Daranciang, M. J. Highland, H. Wen, S. M. Young, N. C. Brandt, H. Y. Hwang, M. Vattilana, M. Nicoul, F. Quirin, J. Goodfellow, T. Qi, I. Grinberg, D. M. Fritz, M. Cammarata, D. Zhu, H. T. Lemke, D. A. Walko, E. M. Dufresne, Y. Li, J. Larsson, D. A. Reis, K. Sokolowski-Tinten, K. A. Nelson, A. M. Rappe, P. H. Fuoss, G. B. Stephenson, and A. M. Lindenberg, Phys. Rev. Lett. **108**, 087601 (2012).

[8] B. Kundys, M. Viret, D. Colson, and D. O. Kundys, Nature Mater. **9**, 803 (2010).

[9] B. Kundys, M. Viret, C. Meny, V. Da Costa, D. Colson, and B. Doudin, Phys. Rev. B **85**, 092301 (2012).

[10] E. M. Dufresne, B. Adams, D. A. Arms, M. Chollet, E. C. Landahl, Y. Li, D. A. Walko, and J. Wang, AIP Conference Proceedings of SRI2009 **CP1234**, 181 (2010).

[11] J. F. Ihlefeld, N. J. Podraza, Z. K. Liu, R. C. Rai, X. Xu, T. Heeg, Y. B. Chen, J. Li, R. W. Collins, J. L. Musfeldt, X. Q. Pan, J. Schubert, R. Ramesh, and D. G. Schlom, Appl. Phys. Lett. **92**, 142908 (2008).

[12] S. R. Basu, L. W. Martin, Y. H. Chu, M. Gajek, R. Ramesh, R. C. Rai, X. Xu, and J. L.

Musfeldt, Appl. Phys. Lett. **92**, 091905 (2008).

[13] A. L. Shluger and A. M. Stoneham, J. Phys.: Conden. Mat. **5**, 3049 (1993).

[14] K. Takahashi, N. Kida, and M. Tonouchi, Phys. Rev. Lett. **96**, 117402 (2006).

[15] C. Korff Schmising, M. Bargheer, M. Kiel, N. Zhavoronkov, M. Woerner, T. Elsaesser, I. Vrejoiu, D. Hesse, and M. Alexe, Phys. Rev. Lett. **98**, 257601 (2007).

[16] R. Berera, R. Grondelle, and J. T. M. Kennis, Photosynth. Res. **101**, 105 (2009).

[17] Y. M. Sheu, S. A. Trugman, Y.-S. Park, S. Lee, H. T. Yi, S.-W. Cheong, Q. X. Jia, A. J. Taylor, and R. P. Prasankumar, Appl. Phys. Lett. **100**, 242904 (2012).

[18] M. D. Biegalski, D. H. Kim, S. Choudhury, L. Q. Chen, H. M. Christen, and K. Do□rr, Appl. Phys. Lett. **98**, 142902 (2011).

[19] D. A. Walko, Y. M. Sheu, M. Trigo, and D. A. Reis, J. Appl. Phys. **110**, 102203 (2011).

[20] R. Shayduk, H. Navirian, W. Leitenberger, J. Goldshteyn, I. Vrejoiu, M. Weinelt, P. Gaal, M. Herzog, C. von K. Schmising, and M. Bargheer, New Journal of Physics **13**, 093032 (2011).

[21] P. Chen, R. J. Sichel-Tissot, J. Young Jo, R. T. Smith, S.-H. Baek, W. Saenrang, C.-B. Eom, O. Sakata, E. M. Dufresne, and P. G. Evans, Appl. Phys. Lett. **100**, 062906 (2012).

[22] J. Seidel, L. W. Martin, Q. He, Q. Zhan, Y.-H. Chu, A. Rother, M. E. Hawkridge, P. Maksymovych, P. Yu, M. Gajek, N. Balke, S. V. Kalinin, S. Gemming, F. Wang, G. Catalan, J. F. Scott, N. A. Spaldin, J. Orenstein, and R. Ramesh, Nature Mater. **8**, 229 (2009).

[23] Y.-H. Chu, M. P. Cruz, C.-H. Yang, L. W. Martin, P.-L. Yang, J.-X. Zhang, K. Lee, P. Yu, L.-Q. Chen, and R. Ramesh, Adv. Mater. **19**, 2662 (2007).

[24] P. Baum, D.-S. Yang, and A. H. Zewail, Science **318**, 788 (2007).

[25] T. Zhao, A. Scholl, F. Zavaliche, K. Lee, M. Barry, A. Doran, M. P. Cruz, Y. H. Chu, C.

Ederer, N. A. Spaldin, R. R. Das, D. M. Kim, S. H. Baek, C. B. Eom, and R. Ramesh, Nature Mater. **5**, 823 (2006).

[26] J. Kreisel, M. Alexe, and P. A. Thomas, Nature Mater. **11**, 260 (2012).

Figure Captions:

Fig. 1 a) θ-2θ scans of the BFO (002) Bragg reflection before and 100 ps after excitation by a 50 fs laser pulse with a central wavelength of 400 nm and the absorbed fluence of 3.2 mJ/cm^2. b) The angular shift Δθ of Bragg peaks and induced strain as a function of delay at various absorbed fluences from 0.67 to 3.47 mJ/cm^2. The solid lines represent fits of a bi-exponential decay. c) The angular shift and induced strain as a function of the pump fluence at 100 ps and 15 ns after the excitation. The solid lines represent linear fits.

Fig. 2 a) Optical absorption spectra in units of the optical density (OD) before (solid) and after (dash) optical excitation of BFO film at absorbed fluence of 3.2 mJ/cm^2. The red curve shows the change in optical density (ΔOD) at 200 ps. b) Transient absorption at 540 nm as a function of delay at various absorbed fluences from 0.37 to 3.2 mJ/cm^2. The solid lines represent the fits using a bi-exponential decay. The inset shows the initial ps dynamics at the absorbed fluence of 3.2 mJ/cm^2.

Fig. 3 a) The dynamics of the induced strain (triangles and diamonds) and optical absorption (solid lines, interpolated from Fig. 2b) at various absorbed fluences from 0.67 to 3.47 mJ/cm^2. b) Strain as a function of the induced absorption at various fluences. The solid lines are linear fits.

Fig. 4 Decomposition of the experimentally observed strain at an absorbed fluence of 3.47 mJ/cm^2 (triangles) into thermal and non-thermal contributions. The red and blue curves are the carrier-induced ($(1-a)S_c(t)$) and thermally induced ($aS_q(t)$) strain respectively. The blue curve is the sum of red and green curves that represents the overall induced strain $S(t)$ upon

photoexcitation.

Wen, *et al*., Figure 1

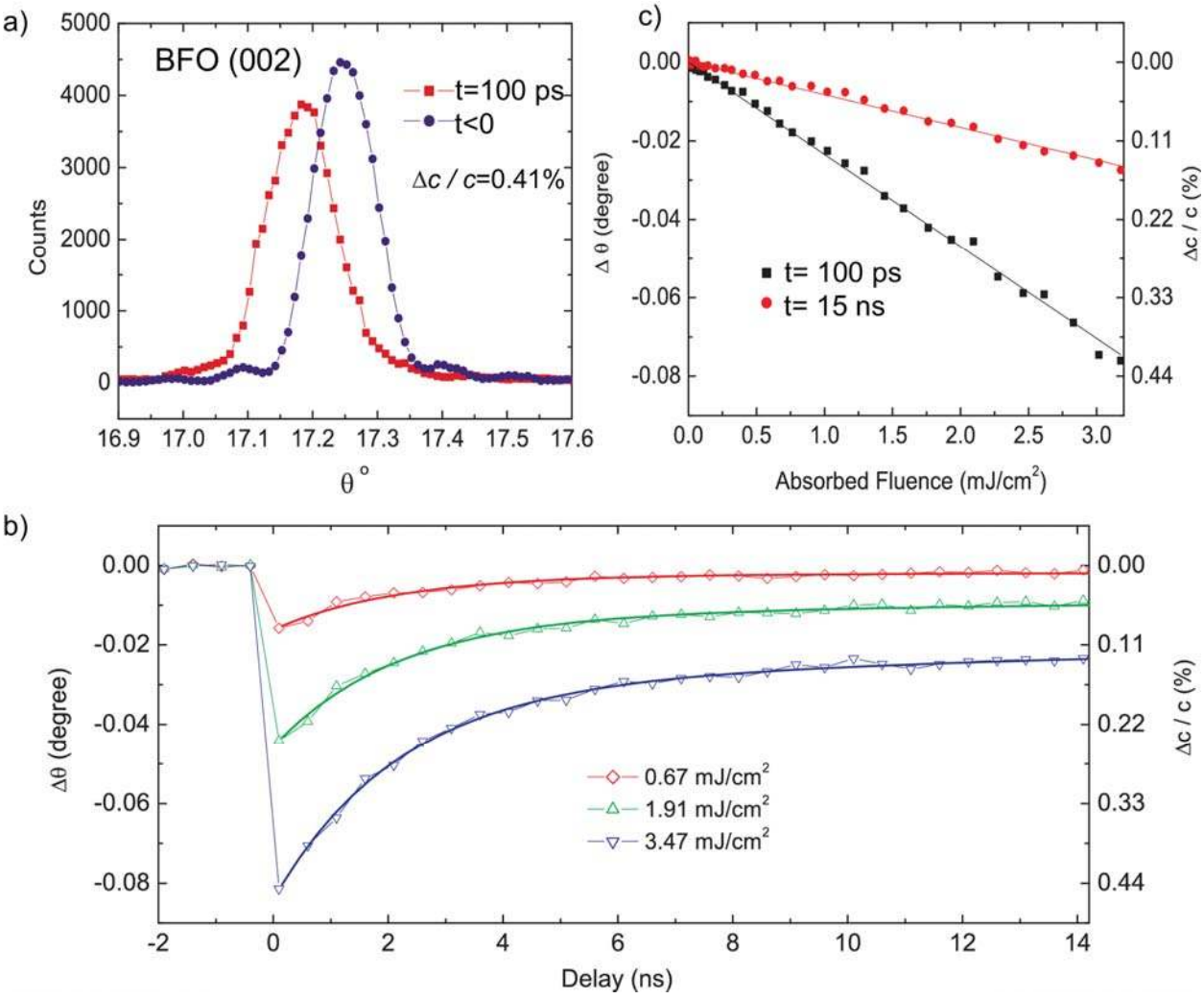

Wen, *et al*., Figure 2

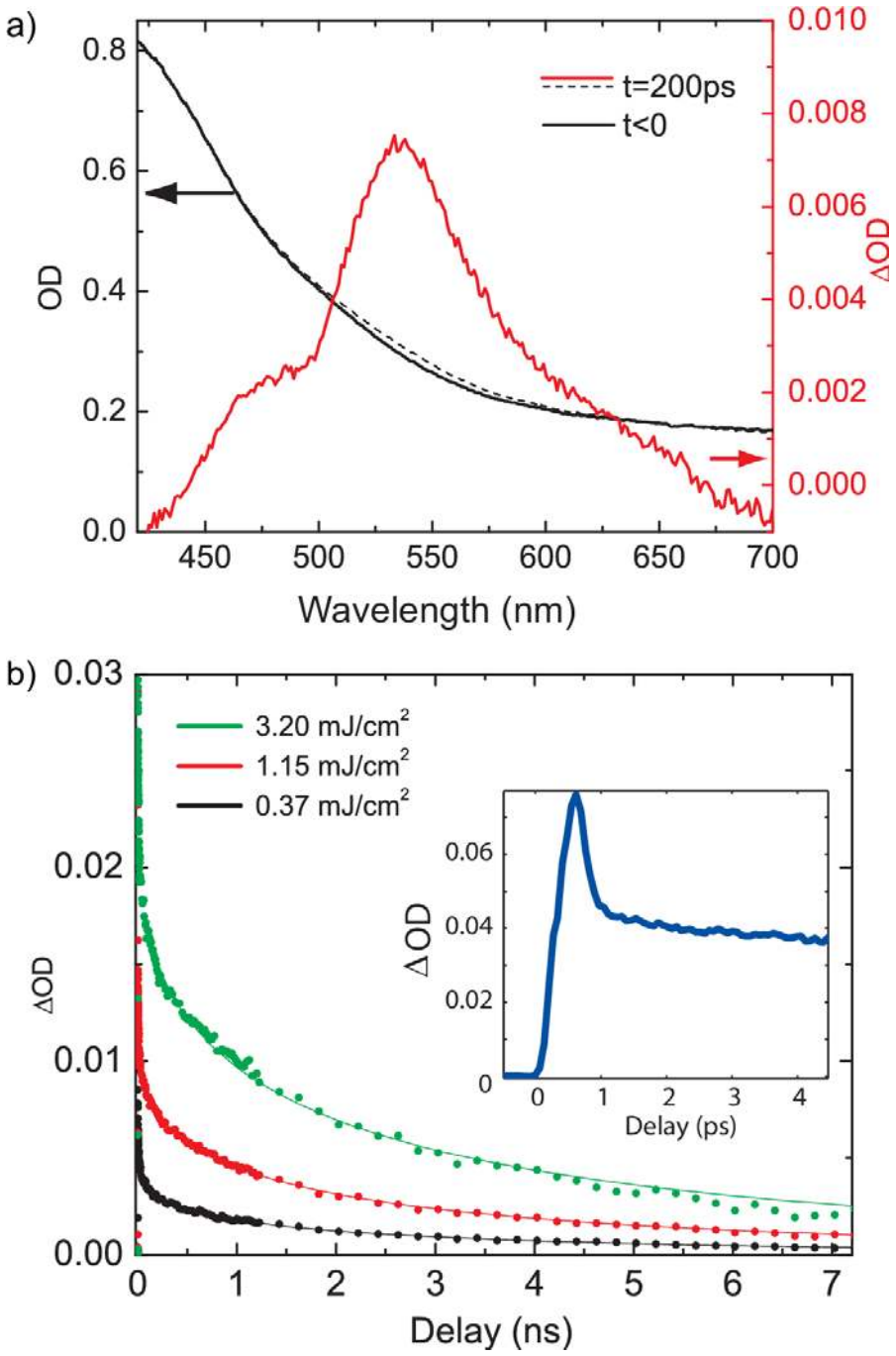

Wen, *et al.*, Figure 3

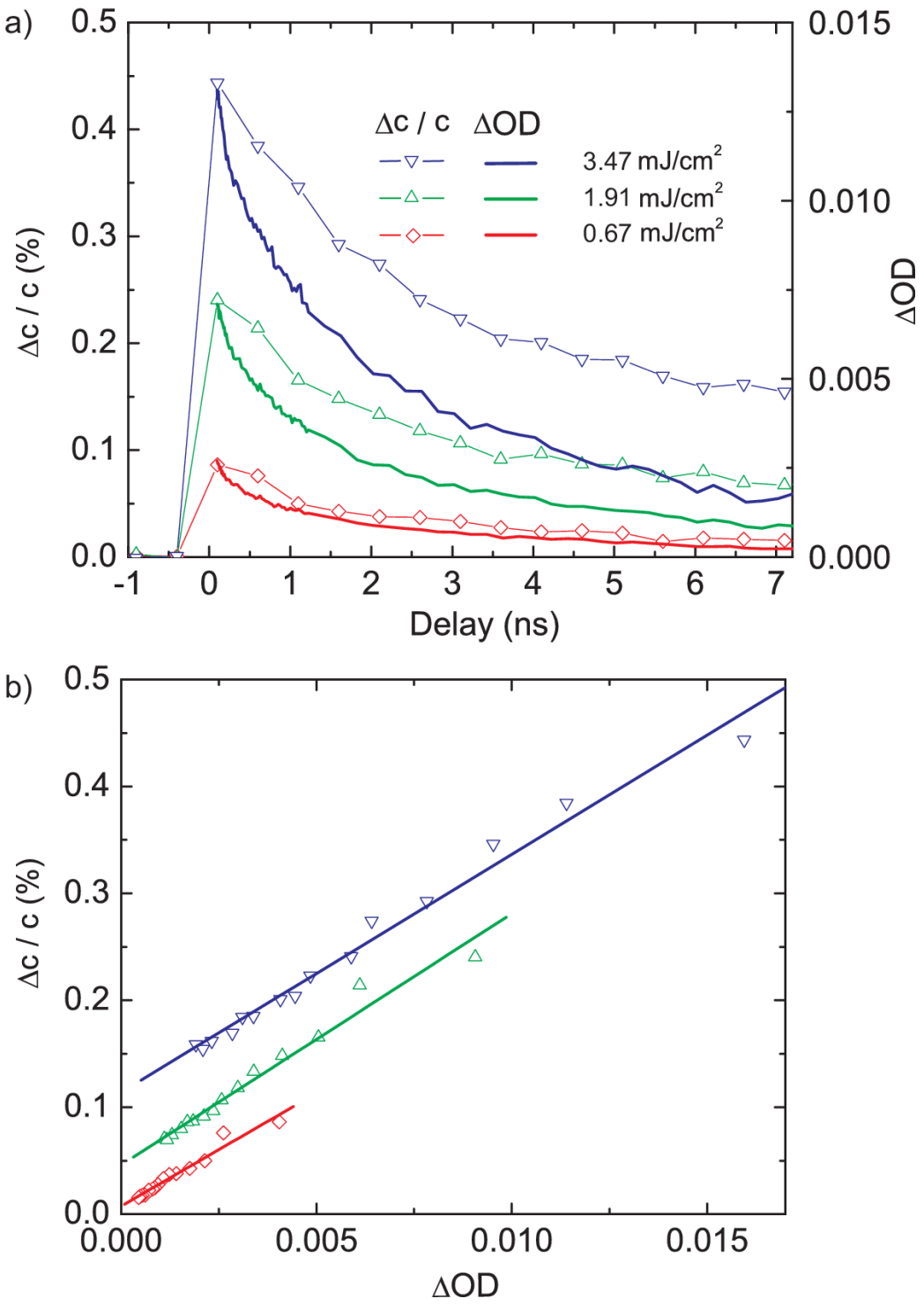

Wen, *et al*. Figure 4